ANNALI DI GEOFISICA, VOL. XXXIX, N. 5, October 1996

Attenuating intensities

Laura Peruzza
C.N.R., Gruppo Nazionale per la Difesa dai Terremoti, at Osservatorio Geofisico Sperimentale, Trieste, Italy

Abstract
The study presents a methodology in which fractile distances for a given macroseismic intensity are used as a point measure on which to do attenuation characterization. The use of statistically derived distances expected not to be exceeded at a given probability avoids ambiguous definition of isoseismal radii, and consequent misinterpretation of attenuation parameters with a physical content. The utility and definiteness of such a fractile distance is evident when treating many earthquakes, of different magnitudes and for which the macroseismic data-sets are of different sizes. The methodology is applied to 55 Italian earthquakes of the last four centuries, with epicentral intensity ranging from VII to XI MCS. Propagation properties in volcanic districts are peculiar, with a rapid decay of observed intensity from the epicentre. The attenuation properties of the other crustal environments are not clearly correlated with the geodynamic domain; the earthquakes show a mean behaviour that appears to depend on relatively homogeneous conditions of propagation. Source depth, tectonic style and finiteness of the source are not addressed because only macroseismic surveying had been applied to most of the earthquakes, and they cannot be linked to surficial fault ruptures. The study is intended to provide mean attenuations that can be used in probabilistic seismic hazard studies; the variability of individual earthquake attenuations for a region introduces the need to use different parameters in future deterministic earthquake scenarios.

Key words *macroseismic intensity – attenuation relationship – seismic hazard*

1. Introduction

Intensity versus epicentral distance relations for earthquakes have been investigated since the beginning of this century. From Köveslighety's (1906) statement of intensity as an energy-like quantity that has to remain constant with respect to space(*), and Cancani's (1904) table of acceleration amplitudes *versus* intensity scale, most authors (*e.g.*, Blake, 1941; Evernden *et al.*, 1973; Ambraseys, 1985) invoke physical constraints on the attenuation model. Two principal types of relationships have been derived. One formulation assumes intensity to be related to the logarithm of energy density (Köveslighety, 1907; Blake, 1941; Karnik, 1969), as expressed in the general equation

$$I = I_0 + a_1 + a_2 \ln \Delta + a_3 \Delta, \qquad (1.1)$$

where Δ represents the hypocentral distance from the focus, and I_0 the epicentral intensity. The other relationship assumes intensity is proportional to the power of energy (*e.g.*, Howell *et al.*, 1975):

$$\ln I = \ln I_0 + b_1 + b_2 \ln \Delta + b_3 \Delta. \qquad (1.2)$$

Some authors simulated intensity (I) attenuation by propagating acceleration (a), via a final a-I conversion (see for example Evernden *et al.*, 1973); others introduced empirical correlations giving a reliable fit on observational data (*e.g.*, Grandori *et al.*, 1987).

Even while recognising the semi-empirical nature of macroseismic intensity, as well as its

Mailing address: Dr. Laura Peruzza, C.N.R., Gruppo Nazionale per la Difesa dai Terremoti, at Osservatorio Geofisico Sperimentale, P.O. Box 2011 (Opicina), 34016 Trieste, Italy; e-mail: lperuzza@ogs.trieste.it

(*) «Si autem intensitas, idest quantitas energiae, ... per axioma conservationis energiae ... facultatem dat solvendi actionis terrae motum in distans».

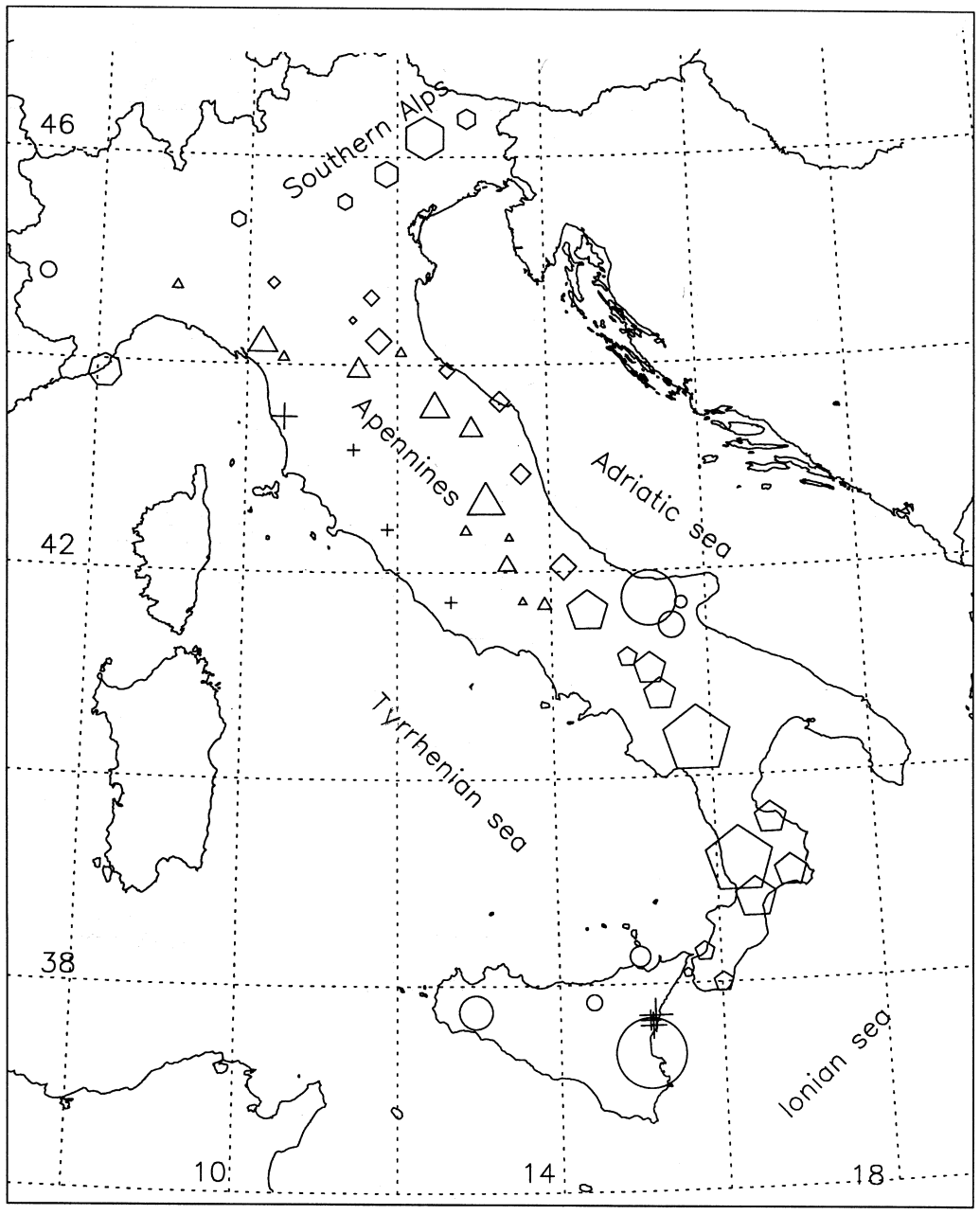

Fig. 1. Epicentre location of the 55 earthquakes treated (from Gruppo Nazionale per la Difesa dai Terremoti, 1994). Symbol sizes are proportional to the I_0 and have the following correspondence to table II: hexagon = A domain (Southern Alps), triangle = B (extensional Apenninic domain), square = C (compressional Apenninic domain), pentagon = E (Southern Apenninic arc), circle = F (foreland domain), heptagon = L (Ligurian sea); D and G volcanic earthquakes are marked with crosses.

non-quantitative definition, the mathematical treatment of intensity values then became more sophisticated (such as inverting the macroseismic field to obtain hypocentre location, computing anisotropy in propagation properties of seismic waves, or evaluating the influence of soil conditions); with the growth in the number of observed intensities, criticism of macroseismic intensity itself increased too.

Often the semi-empirical character of intensity is invoked to supply a non-rigorous treatment of intensity data; the use of intensity scales, the procedures for determining macroseismic parameters (epicentre location, epicentral intensity), the criteria in drawing isoseismal lines, and the manipulation of intensity, disregarding its order-classified variable nature, are often defined subjectively, thus implying a continuous re-evaluation of the meaning and applicability of intensity attenuation relationships. As these relations are widely used in seismic hazard analyses in predicting the intensity expected to be experienced at a given site as a result of an earthquake, only an adequate and codified procedure to compute intensity decay curves, and a proper application of these relations can ensure reliable hazard estimates.

The purpose of this paper is:

a) to present a methodology of using fractile distances for a given macroseismic intensity for fitting macroseismic data points with intensity attenuation relationships;

b) to analyse pitfalls and misunderstandings in the use of attenuation relations, and the possible consequences on some physical quantities derived from attenuation relationships;

c) to comment on propagation characteristics in Italy in the framework of regional attenuation pattern recognition.

The methodology has been applied to 55 Italian earthquakes (Gruppo Nazionale per la Difesa dai Terremoti, GNDT, 1994) with good quality macroseismic data-sets, and epicentral intensities ranging from VII to XI (fig. 1); the total number of intensity points is 9449.

The macroseismic scale used here is the Mercalli-Cancani-Sieberg (MCS), but the arguments may be exported to any other macroseismic scale (*e.g.*, Grünthal, 1993).

2. Methodology

The procedure proposed here characterizes each set of intensities for a given earthquake by a fractile distance. We analyse a macroseismic data-set, *i.e.*, a list of localities with given coordinates and intensity related to an earthquake. The location of the macroseismic epicentre (λ_0, ϕ_0) and epicentral intensity (I_0) correspond to the values reported in the earthquake catalogue, whatever way they have been assessed (this choice will be explained later). The distance of each intensity point from the epicentre is computed according to the basic cartographic rules; points of the same intensity are grouped to define homogeneous populations. Uncertainties in intensity assessment, usually given by the minimum and maximum intensity values (*e.g.*, VII-VIII), are treated by assigning one sample to both the intensity classes with an associated weighting factor. A statistical analysis is then applied to each population, *i.e.*, each intensity class: as distance is a continuous quantity, a cumulative frequency graph (symbols in fig. 2a), and the cumulative density function CDF (lines in fig. 2a), can be calculated according to a chosen probabilistic model. Empirical sample percentiles may also be used instead of those computed under the assumption of a given distribution. Then, the distance expected not to be exceeded at a given probability level is selected. In this way, each intensity class of an earthquake is represented by a single value of distance.

Then, the intensity decay is computed with respect to the epicentral intensity reported in the catalogue as $\Delta I = I_0 - I_{class}$. The use of a numerical axis is invoked, which we call «pseudo-intensity» axis for clearness, where values can be considered numerical, and equidistant: epicentral intensity is thus treated as a number. Finally, the attenuation coefficients of an *a priori* chosen general attenuation equation can be obtained by minimizing predicted-minus-observed pseudo-intensity decay *versus* distance by ordinary algorithms of linear or non-linear fitting (fig. 3 and the following utilise the non-linear Levenberg-Marquardt algorithm, Press *et al.*, 1986).

This treatment does not involve subjective

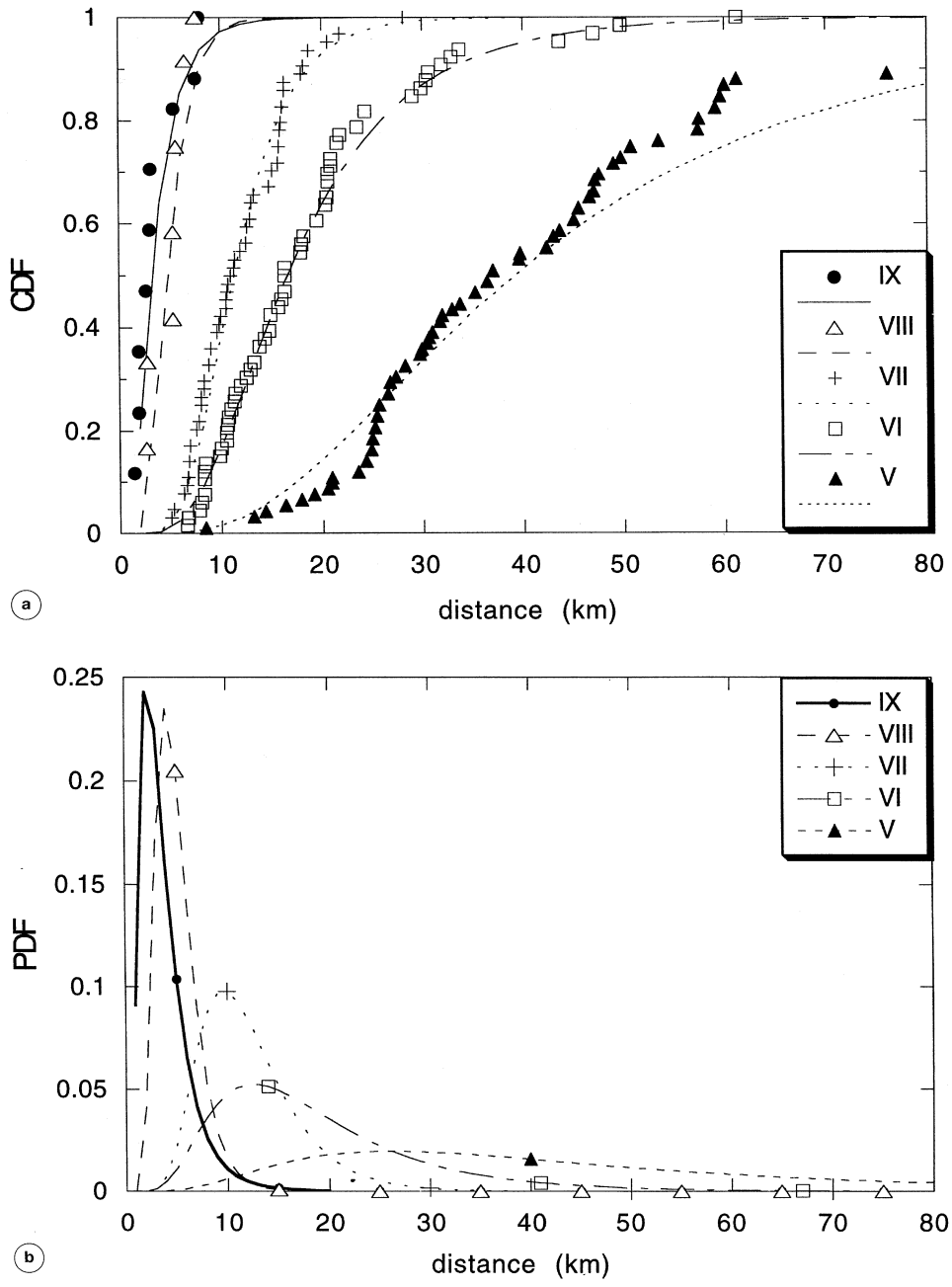

Fig. 2a,b. Statistical graph of the 1928 earthquake data-set: a) cumulative frequency graph of intensity point distances (symbols), and related cumulative density function (CDF, curves); b) probability density functions (PDF) of lognormal distributions represented in (a). The lognormal function is adapted to the sample using the maximum likelihood technique.

isoseismal tracing: on the contrary, the statistical analysis of the intensity class can offer quantitative support for isoseismal radius computation, where the codified criteria of choice is the threshold in probability level (*e.g.*, 80-90%). Fractiles, and not the modal value, should be the most stable available measure of distance attenuation, since they are less sensitive to number of observations.

In theory, every intensity class can exhibit a particular probabilistic model; in practice, the number of observations strongly limits the model choice. The lognormal distribution is here used to treat all the populations in the same way (*e.g.*, fig. 2a,b). The lognormal model, invoked for a phenomenon which arises as a result of a multiplicative mechanism acting on a number of factors (Benjamin and Cornell, 1970), may easily be adapted to an unsymmetrical distribution, such as data often are (fig. 2b). Sometimes the experimental data suggest a bimodal behaviour. Hovewer, after testing (see Peruzza, 1995), the use of bimodal distributions was discarded, because it proved useless for defining the mean attenuations needed in seismic hazard studies. A bimodal behaviour needs at least to be analysed as a function of azimuthal distribution and finiteness of the source, which is beyond the scope of this work.

Figure 3 shows how different attenuation models (*e.g.*, those of Blake, Howell and Grandori) fit the pseudo-intensity decay in almost the same manner; some functional shapes may suit the very short distances from epicentre quite well (Howell model, or Grandori's for example, that does not require null distance for $\Delta I = I_0 - I_{class} = 0$) or the highest distances (Grandori and Blake models), but the flexibility of the parameters can adjust different curves to the same data: the previously pro-

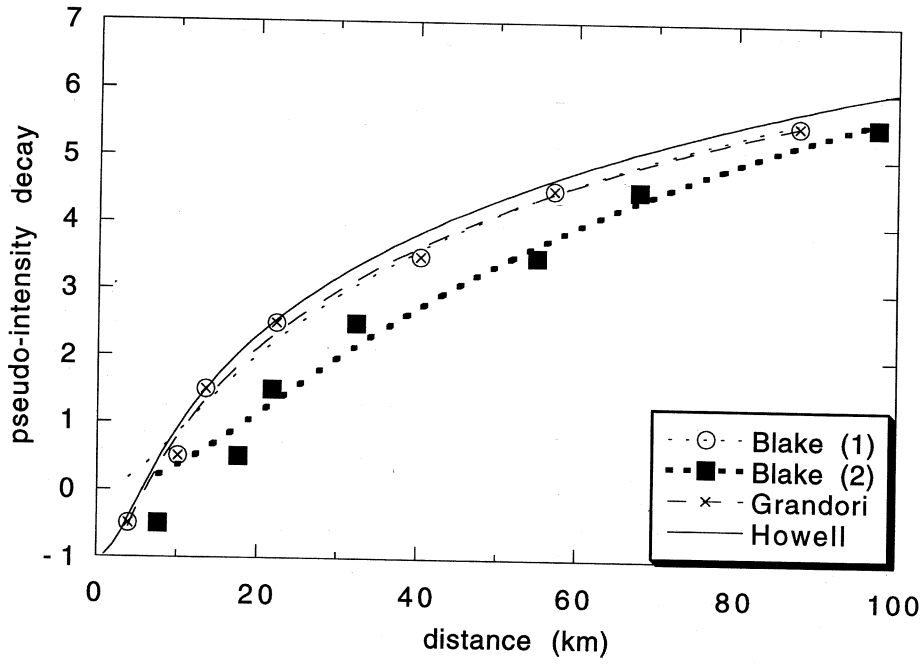

Fig. 3. Curve fitting of intensity attenuation relationships on the 1781 Northern Apennines earthquake. Circles and crosses represent the distance expected not to be exceeded at 50% probability level, and are fitted by three models (Blake (1), Grandori and Howell). Blake (2) model is used also on the black squares, representing the distance expected not to be exceeded at 75% probability. Derived parameters in table I.

Table I. Model type, linear correlation coefficient and values of unknowns of attenuation relationships presented in fig. 3.

Model	R	Coefficients
Blake (1)	0.987	$\alpha = 5.97 \quad h = 10.4$
Grandori	0.997	$\psi = 1.47 \quad \psi_0 = 0.86$ $D_0 = 6.1$
Howell	0.997	$a_2 = 0.46 \quad b_2 = -0.21$ $c_2 = -0.005 \quad h = 4.9$
Blake (2)	0.983	$\alpha = 8.37 \quad h = 21.5$

posed constraints using fractile distances, and the efficiency of the minimisation algorithm, gave very similar correlation coefficients for the different models (see table I).

3. Pitfalls and misinterpretations of attenuation relationships

The previous method proposes a rigid scheme for treating intensity data-sets, where the choice of the type of attenuation model is not of crucial importance. Referring again to fig. 3 and table I, the same attenuation model (Blake) was separately fitted to median and 75-percentile distances; these have different decays, which affect the depth h of the Blake model. Because the original h parameter of Blake has only one definition (*i.e.*, with respect to isoseismal distance) and no standard procedure is given to compute isoseismal distances, the choice of the representative distance value for the intensity class is critical, and the physical meaning (depth of focus in this case) of the attenuation coefficients has to be evaluated carefully, keeping these considerations in mind.

The minimisation is done on a few characteristic values and not by a global treatment of intensity points. The reasons this alternative (*i.e.*, the use of all the data-set coordinates and intensities, where model coefficients and source parameters are unknowns) is not here explored, are the following. Intensities versus distance are very often strongly dispersed, and the fitting algorithms are controlled by the error weighting: high residuals (observed-minus-computed intensity) on a few points of the highest classes are balanced by lower residuals in medium intensity classes, which are usually more completely sampled. Because intensity is considered a numerical value, uncertain intensities build new classes in the middle of the macroseismic intensity scale definition; usually these intermediate classes have fewer samples and force the attenuation curve through the less dispersed, but less reliable observations. Moreover, convergence to a minimum (solution) is sometimes not reached, and frequently depends on the starting values of the unknowns (Howell's formula for example is strongly controlled by the initial guess of the unknowns). These problems are limited by the choice of single values for each intensity class.

The one-class/one-sample approach (following the probabilistic analysis proposed here) is not immune to error either; other possible mistakes are shown in fig. 4a-d. Here a macroseismic data-set and its probability graph are given in separate intensity classes (fig. 4a); the distance corresponding to the median value (horizontal line inside the boxes) is assumed to represent the intensity class, and is fitted by the Blake model (fig. 4b). By minimising the observed-minus-computed intensity (black dots, and dashed line), the epicentral intensity has to be set as unknown: the solution coefficients are $\alpha = 5.52$, $h = 5.32$, $I_0 = 10.59$. The same curve (Obs_I) is reported in fig. 4c with a long dashed line. If this model (with $\alpha = 5.52$, and $h = 5.32$) is applied to the epicentral intensity given in the earthquake catalogue (that is IX-X in this example), the solid curve Obs_Ic of fig. 4c is obtained. The dotted step-wise function (Obs_It) represents the truncation of the computed intensity values, a widely used practice to transform a floating point into an intensity-like integer. As a result of this cycle, the dark dotted boxes of fig. 4d are the intensities predicted by the attenuation model. The method proposed here, starting from the same median values as in fig. 4a, fits the Blake model by considering the intensity decay, with respect to the epicentral intensity given in the catalogue (open circles and solid line in fig. 4b). The

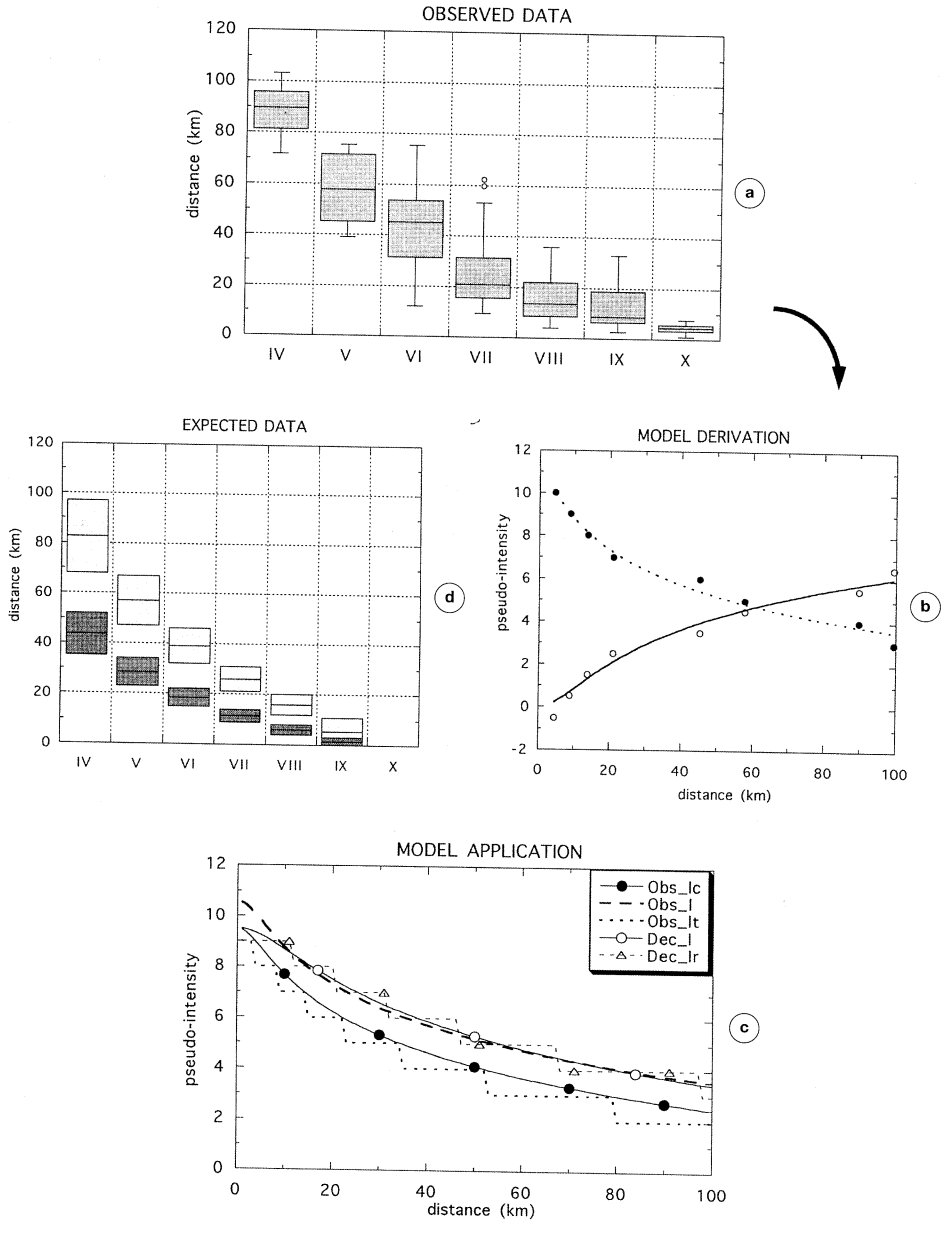

Fig. 4a-d. Description of pitfalls in attenuation modelling. a) Statistical analysis of an earthquake: boxes enclose 50% of data, and the median value is represented by the horizontal line. b) Curve fitting of Blake model on distances corresponding to the median value, for each intensity class: open circles and solid line are pseudo-intensity decay for a given epicentral intensity; black dots and dotted line refer directly to intensity classes as numerical values. c) Attenuation decay curves obtained from (b). d) Expected damage using Obs_It step function (dark boxes) and Dec_Ir (light boxes); see text.

Table II. Studied earthquakes grouped by postulated geodynamic domains. The domains are indicated by capital letters, the events by their date; a code identifies the Grandori curve in the «type» column; the coefficients are also given (standard error in brackets, see the text).

Code	Domain	Events	Type	ψ	ψ_0	D_0
A	Southern Alps	1695/02/25 1802/05/12 1873/06/29 1891/06/07 1928/03/27	all	1.73 (.14)	1.45 (.72)	4.04 (1.4)
			< IX	2.11 (.27)	1.05 (.35)	5.74 (.99)
			≥ IX	1.83 (.09)	1.01 (.18)	3.42 (.34)
B	Extensional Apenninic domain	1703/01/14 1740/03/06 1741/04/24 1781/06/03 1828/10/09 1874/12/06 1898/06/27 1904/02/24 1911/02/19 1919/06/29 1920/09/07 1922/12/29 1958/06/24	all	1.55 (.08)	1.38 (.32)	5.79 (.99)
			< IX	1.66 (.17)	1.44 (.40)	6.12 (1.3)
			≥ IX	1.60 (.09)	1.16 (.37)	5.17 (1.1)
C	Compressional Apenninic domain	1570/11/17 1781/04/04 1916/08/16 1929/04/20 1930/10/30 1933/09/26 1943/10/03 1971/07/15	all	1.46 (.16)	2.32 (2.2)	4.41 (3.1)
			< IX	1.31 (.33)	1.92 (1.9)	9.07 (5.7)
			≥ IX	1.52 (.14)	2.17 (1.5)	3.73 (2.0)
D	Volcanic Tusco-Latial district	1846/08/14 1909/08/25 1927/12/26 1971/02/06	all	1.56 (.21)	1.55 (.67)	3.06 (1.1)
E	Southern Apenninic arc	1638/03/27 1783/03/28 1805/07/26 1832/03/08 1836/04/25 1857/12/16 1894/11/16 1907/10/23 1930/07/23 1962/08/21 1975/01/16 1980/11/23	all	1.55 (.06)	0.87 (.10)	9.23 (.66)
			< IX-X	1.61 (.15)	0.83 (.16)	10.2 (1.1)
			≥ IX-X	1.55 (.06)	0.87 (.12)	8.85 (.77)

Table II (*continued*).

Code	Domain	Events	Type	ψ	ψ_0	D_0
F	Foreland domain	1627/07/30 1693/01/11 1731/03/20 1808/04/02 1875/12/06 1967/10/31 1968/01/15 1978/04/15	all	1.57 (.21)	1.52 (.62)	7.41 (2.2)
G	Volcanic Etnean district	1818/02/20 1894/08/08 1911/10/15	all	–	–	–
L	Ligurian sea	1887/02/23	all	1.45 (.17)	2.59 (3.4)	3.48 (3.7)

loss of one unknown (I_0) simplifies the minimisation; depth and attenuation coefficient ($h = 11.15$, $\alpha = 6.35$) change with respect to model Obs_I, but without a real physical meaning. When the curve (Dec_I in fig. 4c) is retrofitted to the catalogue, and the computed pseudo-intensity is rounded (step-wise line marked as Dec_Ir), attenuation suits the observations better: compare the light dotted boxes of fig. 4d with the original set of fig. 4a. Note also that the two attenuation curves (Obs_I with three unknowns, and Dec_I with two) are very close, diverging only in the first 10 km from the epicentre: the Blake formula requires an epicentral intensity greater than the experimental values, otherwise the maximum observed intensity can never be predicted. Other models (*e.g.*, Grandori) solve this problem.

This example stresses the fact that the damage distribution of macroseismic intensity can be correctly reproduced when the following conditions are satisfied:

a) the attenuation parameters have to be derived by a non-subjective process: the use of fractile distances is a well established quantification of reference distance for computing attenuation curves;

b) the uncertainty in intensity assessment has to be quantified, without building intermediate classes of intensity, which are inconsistent with the original definition of the macroseismic scale; sharing, with a weighting factor, the uncertain data points over several intensity classes guarantees an adequate treatment of uncertainties;

c) the reference point for computing the attenuation relation has to be kept fixed; even if there is poor agreement in the compilation criteria for macroseismic epicentre and epicentral intensity, it is important that attenuation parameters are referred to the same point to which they will be applied; usually this point is the epicentral location and intensity of the record given in the earthquake catalogue;

d) the choice of truncation or rounding when using an attenuation curve has to be declared; otherwise, the real-to-integer transformation can over- or underestimate the computed damage distribution.

4. Application to Italian earthquakes

The methodology was applied to 55 Italian earthquakes (Gruppo Nazionale per la Difesa dai Terremoti, 1994) to find patterns in attenuation characteristics. According to geodynamic considerations (Scandone *et al.*, 1991) the earthquakes are grouped into several domains (see fig. 1 and table II).

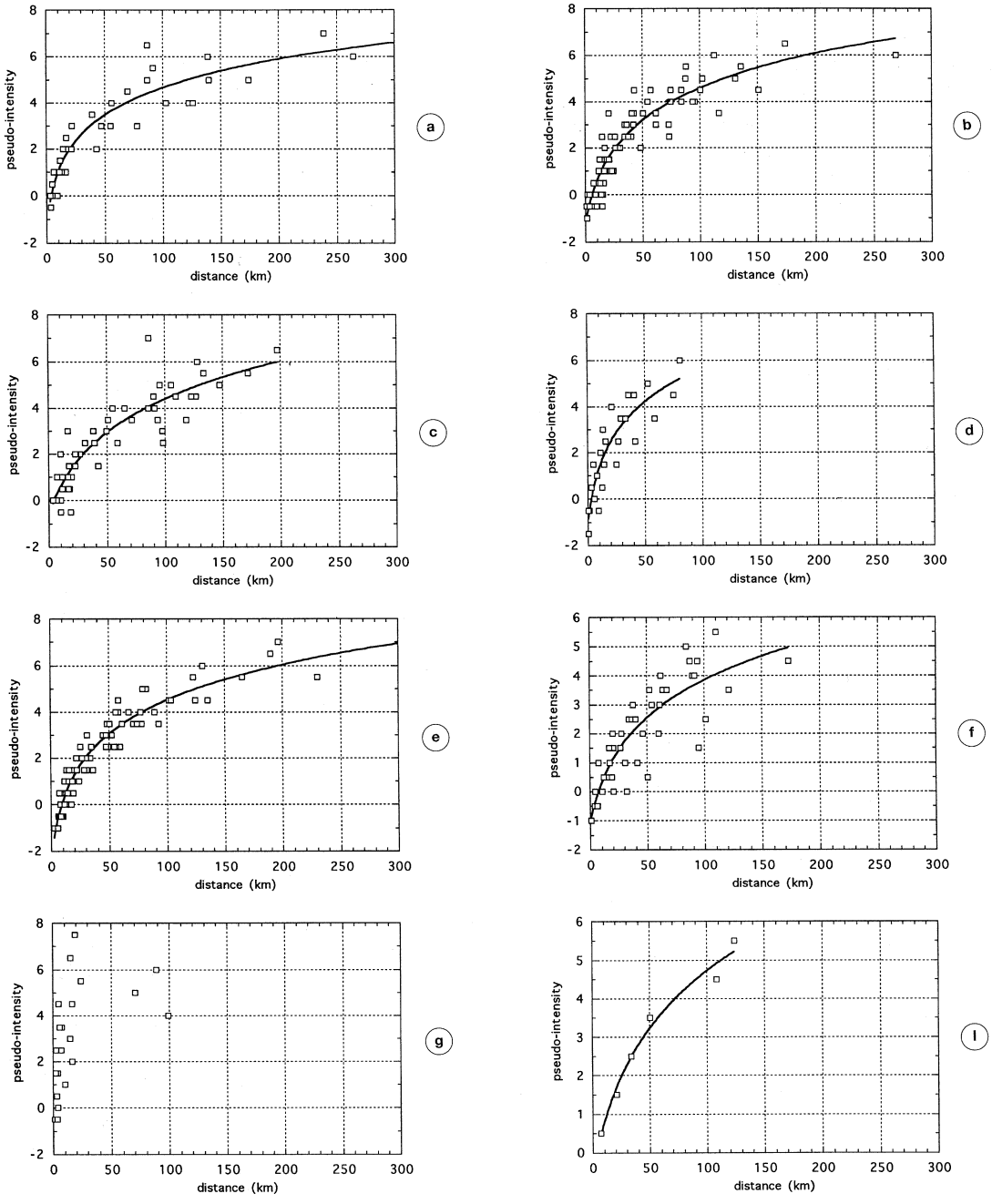

Fig. 5a-g,l. Pseudo-intensity decay *versus* distance, grouping earthquakes according to table II: letters refer to the domain code. Squares are distances expected to be exceeded at 50% probability level; the curve is the Grandori model (type «all» in the table).

For each earthquake, epicentral distances are computed to each intensity point and plotted in cumulative frequency graphs; uncertain intensities are shared by the pertinent classes. The lognormal probabilistic model is then applied to each intensity class. The reference value chosen here corresponds to the distance expected not to be exceeded at 0.5 probability level. The attenuation model given by Grandori *et al.* (1987) is used:

$$I_0 - I_i = \frac{1}{\ln \psi} \ln \left[1 + \frac{\psi - 1}{\psi_0} \left(\frac{D_i}{D_0} - 1 \right) \right], \qquad (4.1)$$

where D_i is the epicentral distance of the i_{th} intensity class; D_0, the radius of the zero-decay isoline, ψ and ψ_0 are the unknowns to be solved by fitting the pseudo-intensity decay versus distance.

This model is preferred for its flexibility at short and long distances, as described in fig. 3; the decay of intensity can be negative when I_0 (epicentral intensity, taken from the catalogue) is lower than I_{max}. Graphic display of samples and curve fitting is given in fig. 5a-g,l.

As previously stated, earthquakes are grouped according to table II. The resulting Grandori coefficients with the relative standard errors are also reported in table II. Because fractile distances introduce an artificial reduction of variance intrinsic to the observed data, the errors are underestimated, and can only be considered a comparison. No curve fitting was done for the volcanic G domain (fig. 5g), where samples are few and some are very scattered: moreover the decay is very sharp, suggesting a linear, more than logarithmic dependence on distance. The area L is represented by one earthquake only (fig. 5l), and the domain coefficients are a set of «single event» coefficients. When the Grandori curves are plotted together (fig. 6), there is no meaningful difference in attenuation characteristics, with the exceptions of group D (volcanic district), where

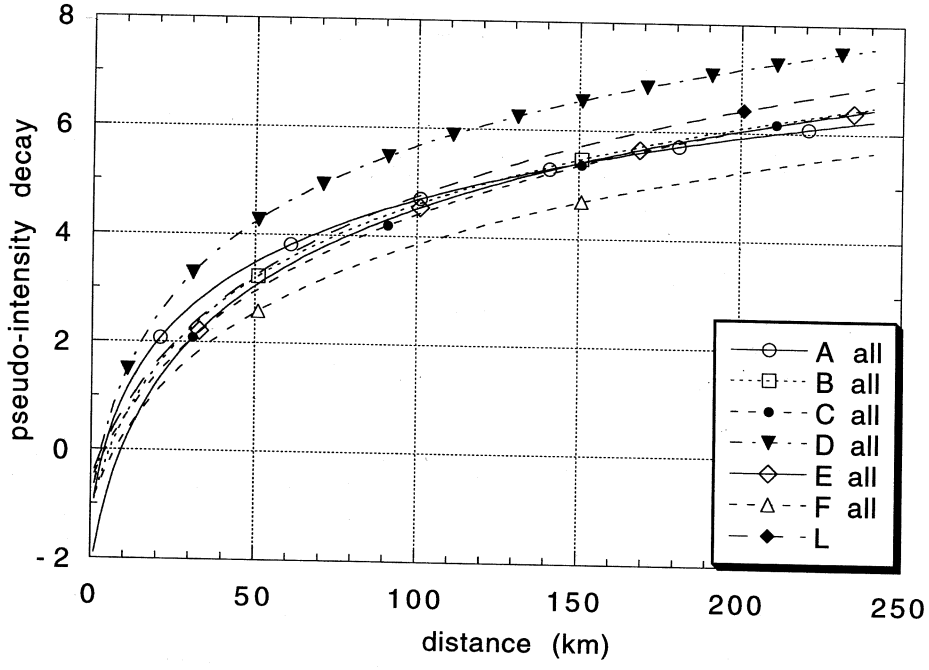

Fig. 6. Attenuation curves of the different geodynamic domains derived from fig. 5.

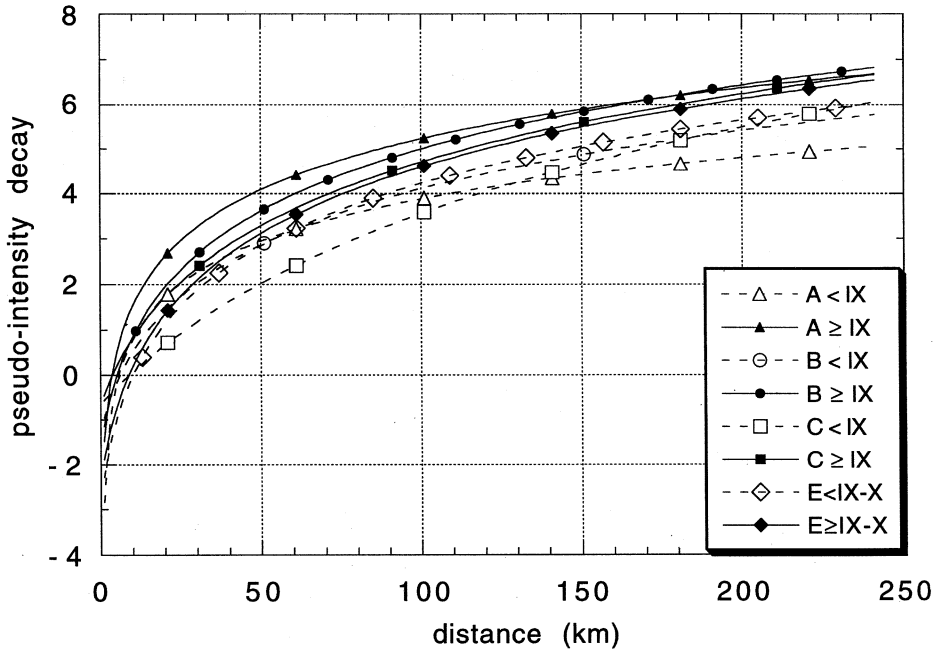

Fig. 7. Attenuation curves of geodynamic domains, splitting the earthquakes into two groups, according to their epicentral intensity (see table II).

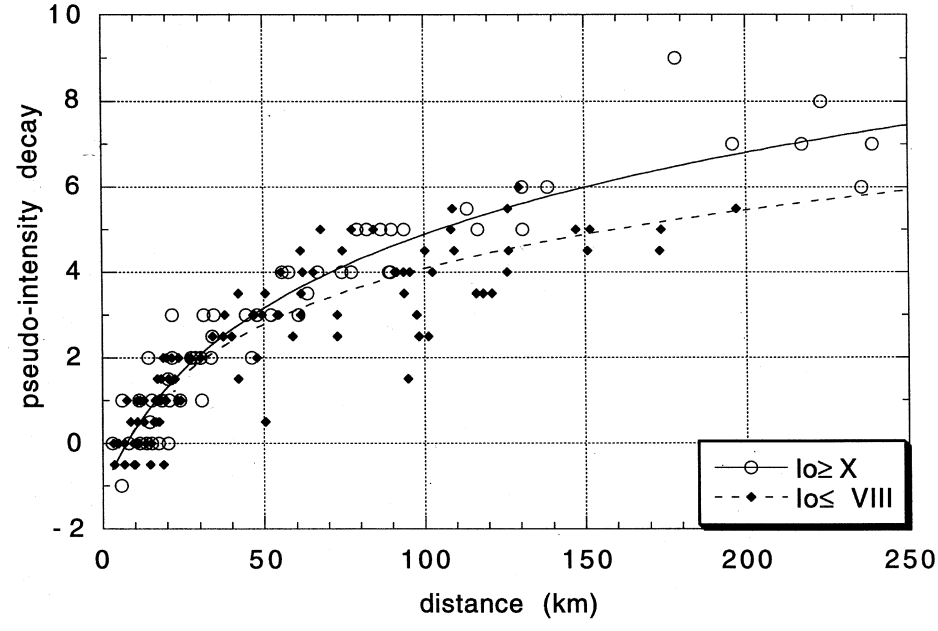

Fig. 8. Pseudo-intensity decay *versus* distance of earthquakes with $I_0 \geq$ X MCS (open circles) and $I_0 \leq$ VIII (black squares) and related curve fitting.

the propagation is lower, and zone F which shows some evidence of a higher propagation. The first case is supported by the other volcanic zone (fig. 5g) which has the same tendency, even if it gave no results. The propagation in zone F seems less reliable; in fig. 5f, two separate attenuation trends can be recognized.

The Grandori coefficient values (in table II) are not directly representative of the attenuation characteristics. Different combinations of ψ, ψ_0 and D_0 give approximately the same curves: to define an attenuation curve, the coefficients have to be kept together, in contrast to the common coefficient interpretations. The non-uniqueness of the Grandori parameters means that the analysis of attenuation characteristics by separately mapping the values of one single coefficient can be unrealistic, and no regional averaging of parameters can be performed.

According to the results of Grandori *et al.* (1987, 1988) on the attenuation dependence on epicentral intensity, the earthquakes of each domain were treated again, splitting the events into two groups according to their epicentral intensity I_0. The resulting curves are plotted in fig. 7, and the coefficients are reported in table II again. In domains A, B and C, the «low I_0 group» (dashed curves) consists of events with $I_0 <$ IX MCS, the «high I_0 group» (solid lines) with $I_0 \geq$ IX earthquakes. In the E domain, where the earthquakes are stronger, the limit between the two groups was raised to IX-X. Domains D and F were not treated, because grouping with respect to I_0 did not decrease the sample dispersion. Figure 7 suggests a certain dependence of the propagation properties on I_0, while the structural domains again remain indistinct. Curves related to the low I_0 group are separated from the high I_0 family, from distances greater than 30 km, and intensity decay greater than 2. Intensities decay more rapidly when the earthquake is stronger, with an average decay of 5 at 100 km distance, while a decay of 4 at 100 km is expected for a low I_0 event. This contrasts with what Grandori *et al.* (1987, 1988) stated; moreover, the correlation, proposed by those authors, between the attenuation dependence on I_0 and D_0 is incompatible with the previous considerations on the non-uniqueness of the parameters, and is disproved also by the experimental data (see table II).

The complexity of an I_0-dependent attenuation in fig. 7 is analysed again in fig. 8. All the earthquakes (excluding the volcanic area events) were re-grouped according to their I_0 only, to obtain a statistically more meaningful number of events. The two extreme groups of $I_0 \geq$ X and $I_0 \leq$ VIII are plotted in fig. 8, with the relative curve fitting. The two attenuation curves diverge for distances greater than 50 km, with a definite difference of more than one intensity unit at 100 km, but the sample distributions (open circles and filled squares) overlap widely: their dispersion increases from 20 km at 0 pseudo-intensity decay, to about 80 km for a decay of 4. The low I_0 events are the most scattered; further analyses on data sampling problems (for example the meaningfulness of data points at the limit of perceptibility) and a more adequate quantification of earthquake «size» (for example macroseismic magnitude in the sense of Westaway, 1992) will probably help to solve some of these uncertainties. Currently, the I_0-dependence of mean attenuation on a point source cannot be satisfactory resolved in the first 100 km; this result is qualitatively equivalent to the independence of peak ground acceleration decay from magnitude, established by experimental relationships (see Campbell, 1985 for a review).

Finally, the variability in attenuation of individual earthquakes for a region is investigated: fig. 9 represents the «single event» attenuation curves for 12 earthquakes of domain B; the earthquakes are listed in the legend with decreasing I_0. The average model of fig. 5b is also plotted with a thick line. The graph illustrates how the mean attenuation curve derived from a subset of 12 earthquakes averages different attenuation trends. Most of the curves lie in one intensity unit interval, while three events (1922, 1874 and 1828) have stronger propagation characteristics and one (1904) is rapidly attenuated. No reliable assumptions on depths of focus, or tectonic styles are possible for all these events, but the definition of single event curves addresses the issue of using attenuation parameters to guess future deterministic

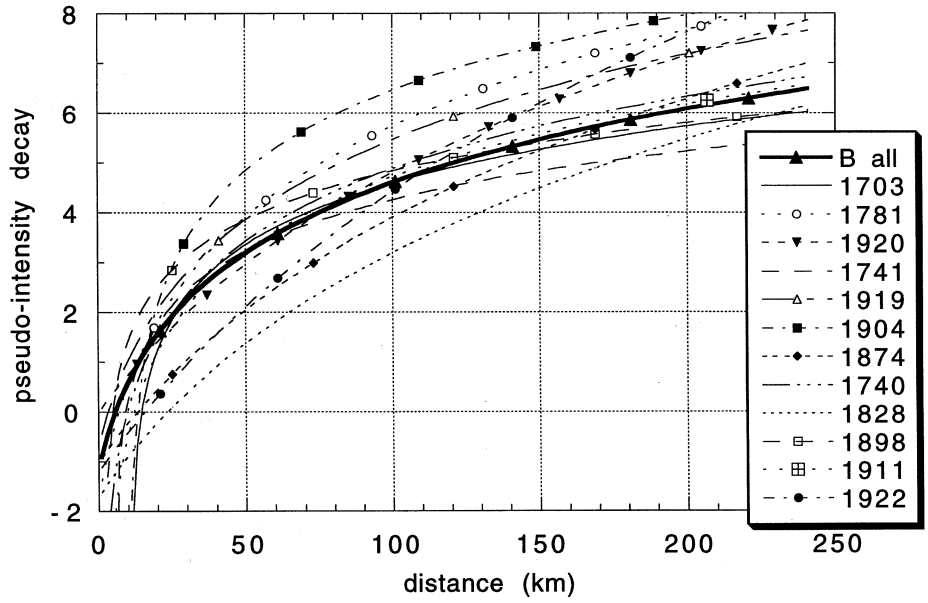

Fig. 9. «Single event» attenuation curves for the extensional Apenninic domain B; thick line represents the global curve of fig. 5b.

earthquakes; their homogeneity with respect to focal mechanisms and hypocentral parameters has to be tested on earthquakes which have been both macroseismically and instrumentally monitored.

5. Conclusions

Methodological and practical conclusions arise from the present analysis.

Concerning the methodology, the procedure developed codifies the criteria for macroseismic data-set analysis, by defining a treatment for the uncertain data and the way of deriving a distance reference value for the intensity classes: by using fractile distances, elaboration of intensity data-sets becomes transparent, and different propagation models can be applied and tested.

The physical meaning given to some attenuation parameters has to be carefully evaluated: they are often non-unique and strongly dependent on ambiguous definitions. An efficient reproduction of damage distribution requires consistency between attenuation coefficients and epicentral parameters.

The Grandori attenuation model is flexible enough to reproduce intensities greater than the epicentral intensity through the D_0 parameters. The dependence of attenuation on I_0 proposed by those authors is controversial: in any case, it is not governed by variation in the D_0 parameter.

Mean attenuations and their variability derived with the present method are useful in seismic hazard studies; the point source assumption is acceptable in this context.

Considering the Italian area, the volcanic districts show a lower propagation of intensity versus distance, which is physically consistent with the shallower seismicity expected in volcanic areas. Working on a statistically meaningful number of earthquakes, the mean attenuation curves of other geodynamic domains are relatively homogeneous, with global dispersion over a range of about 2 intensity degrees at

20 km from the epicentre, and 4 at 100 km. Grouping the events in relation to their I_0, the attenuation curves diverge for large distances, but are not distinctive in the first 100 km. The variability of individual earthquake attenuations introduces the need to use different parameters in future deterministic earthquakes.

Acknowledgements

The research was undertaken within the framework of CNR's GNDT activities. I wish to thank David Perkins who gave helpful and prompt comments to improve the first version.

REFERENCES

AMBRASEYS, N.N. (1985): Intensity-attenuation and magnitude-intensity relationships for northwest European earthquakes, *Earthquake Eng. Struct. Dyn.*, **13**, 733-778.

BENJAMIN, J.R. and C.A. CORNELL (1970): *Probability, Statistics, and Decision for Civil Engineers* (McGraw-Hill, New York), pp. 684.

BLAKE, A. (1941): On the estimation of focal depth from macroseismic data, *Bull. Seismol. Soc. Am.*, **31**, 225-231.

CAMPBELL, K.W. (1985). Strong-motion attenuation relations: a ten-year perspective, *Earthquake Spectra*, **1**, 759-804.

CANCANI, A. (1904): Sur l'empoi d'une échelle sismique des intensités, empirique et absolute, in *Verhandl. d. zweiten Internat. Seismol. Konferenz, Leipzig*, 281-283.

EVERNDEN, J.F., R.R. HIBBARD and J.F. SCHNEIDER (1973): Interpretation of seismic intensity data, *Bull. Seismol. Soc. Am.*, **63** (2), 399-422.

GRANDORI, G., F. PEROTTI and A. TAGLIANI (1987): On the attenuation of macroseismic intensity with epicentral distance, in *Ground Motion and Engineering Seismology*, edited by A.S. CAKMAK, Delopments in Geotechnical Engineering, **44** (Elsevier, Amsterdam), 581-594.

GRANDORI, G., A. DREI, E. GARAVAGLIA and C. MOLINA (1988): A new attenuation law of macroseismic intensity, *Ninth World Conference Earthquake Engineering*, Tokyo, A03-01.

GRÜNTHAL, G. (Editor) (1993): European Macroseismic Scale 1992 (up-dated MSK-Scale), Conseil de l'Europe, *Cahiers du Centre Europeen de Geodynamique e de Seismologie*, Luxembourg, **7**, 79.

GRUPPO NAZIONALE PER LA DIFESA DAI TERREMOTI (1994): *Macroseismic Intensity Database*, Milano.

HOWELL, B.F. and T.R. SCHULTZ (1975): Attenuation of modified Mercalli intensity with distance from the epicenter, *Bull. Seismol. Soc. Am.*, **65** (3), 651-666.

KARNIK, V. (1969): *Seismicity of the European area/I* (Reidel Publ. Co. Dordrecht), pp. 364.

KÖVESLIGETHY VON, R. (1906): Seismonomia, *Boll. Soc. Seismol. It.*, **11**, 113-250.

KÖVESLIGETHY VON, R. (1907): Seismischer Stärkegrad und Intensität der Beben, *Gerlands Beitr. Geophys.*, **8**, 363-366.

PERUZZA, L. (1995): Macroseismic intensity versus distance: constraints to the attenuation model, in *Soil Dynamics and Earthquake Engineering VII*, edited by A.S. CAKMAK and C.A. BREBBIA (Comp. Mech. Publ., Southampton), 215-222.

PRESS, W.H., B.P. FLANNERY, S.A. TEUKOLSKY and W.T. VETTERLING (1986): *Numerical Recipes* (Cambridge University Press).

SCANDONE, P., E. PATACCA, C. MELETTI, M. BELLATALLA, N. PERILLI and U. SANTINI (1991): Struttura geologica, evoluzione cinematica e schema sismotettonico della penisola italiana, in *GNDT, Atti del Convegno 1990. Zonazione e Riclassificazione Sismica* (Tip. Moderna, Bologna), vol. 1, 119-133.

WESTAWAY, R. (1992) Seismic moment summation for historical earthquakes in Italy: tectonic implications, *J. Geophys. Res.*, **97**, 15437-15464.